J Mater Sci (2009) 44:1750–1756
DOI 10.1007/s10853-009-3290-5

Processing and characterization of MWCNT reinforced aluminum matrix composites

I. Sridhar · Karthic R. Narayanan

Received: 27 May 2008 / Accepted: 21 January 2009 / Published online: 18 February 2009

Abstract Metal matrix composites comprising aluminum matrix and multi-wall carbon nanotubes (MWCNTs) as reinforcements are fabricated using cold uniaxial compaction followed by sintering and cold extrusion as secondary processes. The MWCNTs are pretreated with sodium dodecyl sulfate for improved adhesion with aluminum powder. The effect of sintering temperature on the microstructure is explored using differential scanning calorimetric spectrum. The tensile yield and ultimate strength of Al-MWCNTs increased to 90% with 2 wt% addition of MWCNTs. Various theories for the strengthening and stiffening of Al-MWCNTs composites are explored.

Introduction

Carbon nanotubes (CNTs), discovered by Iijima, are one of the most exciting nanostructural materials of the 20th century due to their superior mechanical, thermal, and electrical properties [1–3]. Theoretical and experimental investigations on CNTs have reported their Young's modulus and tensile strength to be of the order of 3 TPa and 2 GPa, respectively [4–9]. Their excellent mechanical properties combined with their nano-size and low density of 2.0 g/cm^3 makes them as a viable reinforcing phase in a variety of polymer, ceramic, and metallic matrices to design high-performance composite materials. Aluminum alloys are widely used in aerospace, automotive industries as they possess low density, capable of being strengthened by precipitation hardening, have good corrosion resistance, high thermal and electrical conductivity [10]. CNTs could be an ideal reinforcing phase to design aluminum matrix composites (AMCs) to improve Al alloys wear and creep resistance. Recent research on producing Al matrix composites reinforced with CNTs has been based on near net-shape routes, such as cold compaction, melt deposition, cold isostatic pressing, hot roll compaction, etc., for the primary processing followed by (in some cases) secondary process like hot extrusion to further enhance the properties of the metal matrix composites [11–16]. In a recent paper, Loo et al. [17] have fabricated multi-wall carbon nanotubes (MWCNT) reinforced silica composites using sol–gel route and they have outlined the importance of surface treatment of MWCNTs for their effective dispersion. To the best of authors' knowledge, the current experimental data on Al-MWCNTs are still very much limited and that too cold extrusion processing is not explored. Hence, the aim of this paper is to compare the enhancement in mechanical properties of aluminum matrix composites reinforced with different weight percentages (0.5, 1.0, and 2.0) of chemically treated MWCNT to the monolithic 99.96% pure aluminum fabricated by cold compaction as a primary process followed by sintering and cold extrusion as secondary processes. The secondary process involved here is economical when compared to the initial expenditure involved in some of the net shape forming routes like spark plasma sintering and hot isostatic pressing. Various theories for the strengthening and stiffening of Al-MWCNTs composites are also explored. To date the MWCNTs are much cheaper than single-wall carbon nanotubes (SWCNTs) and hence we will be using MWCNTs in the current experimental studies for cost-effectiveness.

I. Sridhar · K. R. Narayanan (✉)
School of Mechanical & Aerospace Engineering,
Nanyang Technological University, 50 Nanyang Avenue,
Singapore 639798, Singapore
e-mail: re0002an@ntu.edu.sg

Materials and methods

The aluminum (Al) powder used is pure Al (99.6 wt% Al) produced by argon gas atomization supplied by Alfa Aesar, Germany. The Al powder has nearly spherical shape particles with many satellite sub-particles with an average particle size (APS) of 20–30 μm. A micrograph of the aluminum powder obtained using scanning electron microscopy (SEM) is shown in Fig. 1a. The MWCNTs were produced by the catalytic pyrolysis of methane and supplied by Shenzen Nano Tech Port Co. Ltd, China. The MWCNTs have a nominal diameter of 10 nm, length of 5–15 μm, and surface area of 40–300 m^2/g. The micrograph of MWCNTs obtained through field emission scanning electron microscopy (FESEM) is shown in Fig. 1b. The FESEM image shows that the CNTs tend to clump together due to van der Walls force of attraction between them.

Surface treatment of MWCNTs

Raman spectroscopy with He:Ne laser of 633 nm wavelength was used to characterize the MWCNTs obtained from the manufacturer [18, 19]. The spectrum of MWCNTs showed a disorder (D-band) at 1348 cm^{-1} and tangential G-band at 1590 cm^{-1}, respectively. This G-band Raman shift confirmed the presence of amorphous carbon (<3 wt%) as stated by the manufacturer. The MWCNTs are first cleaned by distilled (DI) water and then surface-treated before mixing with aluminum powder. Initially, MWCNTs are sonicated for 4 h in 63 vol.% nitric acid and filtered. The filtered acidic MWCNTs are neutralized with sodium hydroxide solution, and then dried by heating them in an oven at 110 °C for 2 h. Finally for better adhesion between the MWCNTs and Al powder, they were treated with sodium dodecyl sulfate (SDS) surfactant, which decreases the van der Walls force of attraction between the MWCNTs [20, 21]. Two grams of SDS was dissolved in 200 mL of water. The nanotubes were added to the SDS solution and sonicated for 4 h. These treated nanotubes were filtered and baked at 110 °C for 2 h for drying. When ionic SDS is used as the surfactant, the negative charges in SDS micelles that absorb on MWCNTs prevent re-aggregation of MWCNTs.

Composite preparation

Initially, required amount of Al powder and surface-treated MWCNTs were transferred to a horizontal blending machine which had air tight metallic containers. The powders were mechanically mixed for about 2 h in the blender set at 200 rpm. Previous work showed that the mixing process and its duration determine the effective dispersion of MWCNTs in the powder [22]. Measures were taken to prevent the loss of powder mixture during blending. After blending immediately the monolithic Al and MWCNT reinforced Al, specimens were produced using cold uniaxial pressing in a 25 ton hydraulic press, which can provide the manufacturer suggested 2 ton/cm^2 compaction pressure. The cold-pressed cylindrical specimen are 18 mm in diameter and 30 mm in length. These green compacts are then free-sintered at a heating rate of 10 °C per minute up to 580 °C (based on 660 °C melting temperature of Al powder) in a furnace maintained for 90 min and then cooled to room temperature at a rate of 3 °C per minute in the furnace itself. Finally, the sintered specimens are extruded in a hot-tool steel die of 45° die angle at room temperature to 12 mm diameter and length of 45 mm using the same 25 ton hydraulic press. The extrusion load was calculated to be 22.8 ton with an equivalent plastic strain of 0.81. The reduction in area was 55.55% and extrusion ratio was 2.25. The initial sintering temperature was set to 580 °C as adopted by George et al. [12] in their Al-MWCNT composites fabrication by hot extrusion. The differential scanning calorimeter (DSC) spectrum of these Al-MWCNT composites in Fig. 2a shows an exothermic peak after aluminum melting point, indicating the formation of Al_4C_3 (aluminum carbide) phase between the Al and MWCNT interface. The presence

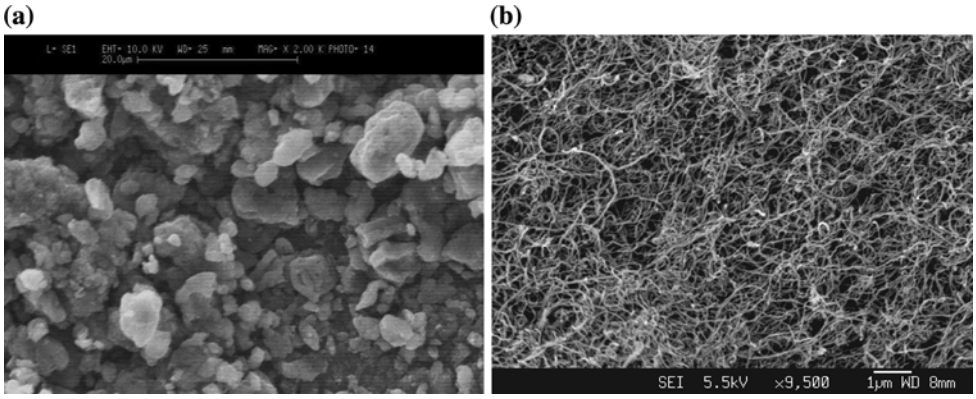

Fig. 1 **a** Scanning electron micrograph of aluminum powder and **b** field emission micrographs of MWCNTs

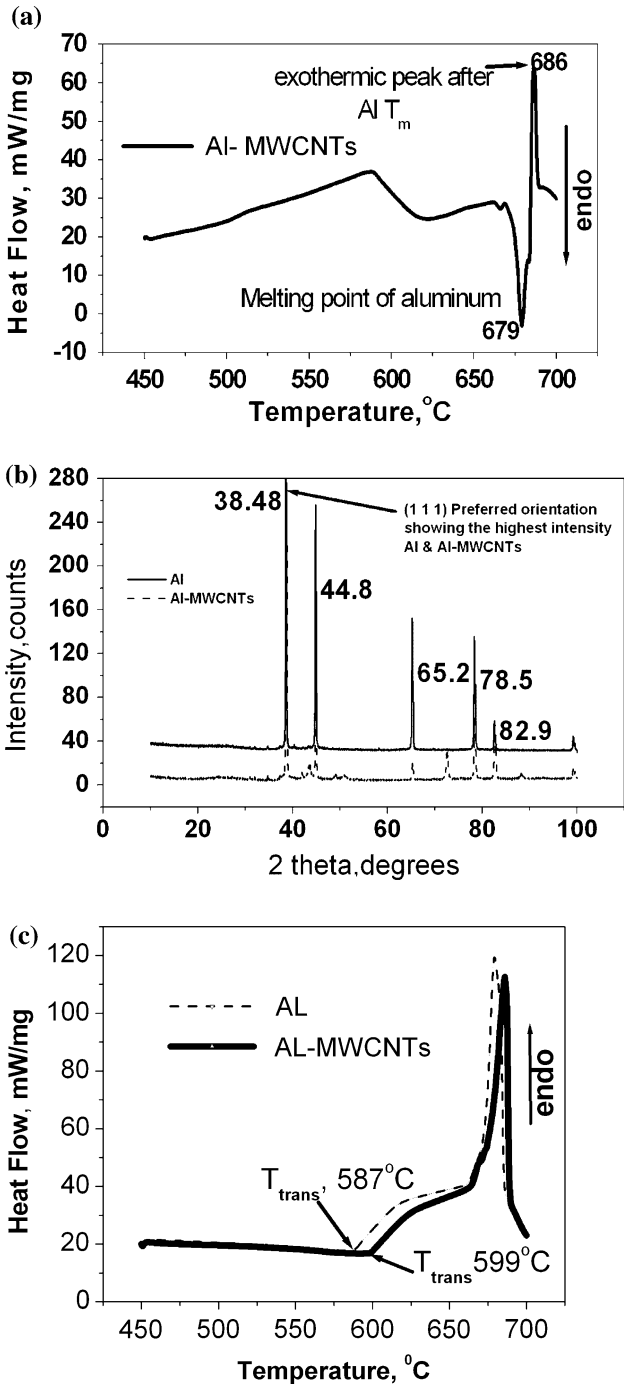

Fig. 2 **a** DSC spectrums for AL-MWCNTs sintered at 580 °C, **b** XRD spectrum of Al and Al-2 wt% MWCNT composite, and **c** DSC spectrum for Al and Al-MWCNT composite sintered at 520 °C

of interfacial compound aluminum carbide deteriorates composite properties. Hence, the sintering temperature was reduced to 520 °C and the X-ray diffraction (XRD) spectrum of Al and Al-MWCNT composites shown in Fig. 2b confirmed the absence of aluminum oxide as well as aluminum carbide as their reference peaks were absent. The DSC curves in Fig. 2c indicate the effect of MWCNTs over the transition temperature (T_{trans}) of AMCs compared to pristine Al, which shows that the strength of the Al-MWCNT composite is retained for longer periods. The optimal sintering temperature needs to be further investigated as Jiang et al. [23] have highlighted the careful selection of sintering temperature in designing CNT reinforced alumina composites.

Results

Density and microstructural analysis

The densities of the extruded Al and Al-MWCNT composites were measured by the Archimedes principle with deionized water as the immersion medium and are listed in Table 1. The extruded samples density increased with increasing MWCNTs weight percentage. This unexpected result is against the rule of mixtures given that the density of MWCNTs is less than that of Al. Similar trend is also reported in the literature [11–14] for CNT reinforced MMCs. The role of porous MWCNTs in controlling the densification is beyond the scope of this paper. The density gradient along the length of the specimen was less than 2%. The extruded Al-MWCNT composites have a smooth surface finish as shown in Fig. 3a. The microstructure of the specimen along the extruded direction showed that large percentage of grains are oriented along the extrusion direction as shown in Fig. 3b and c and a homogeneous bridging of MWCNTs in the matrix was evident. The microstructure indicated some preferential alignment of MWCNTs perpendicular to the extruded direction. Further, the grain structure has certain anisotropy as a result of the lateral deformation constraint provided by the extrusion die. The grain size (shown in Fig. 3d) after extrusion decreased due to high strain rate applied in the cold extrusion process.

Mechanical characterization

The mechanical micro and macro properties of composites were obtained by microhardness testing and uniaxial tensile tests. The microhardness test was carried out in a CSM^{TM} microhardness tester using a Berkovich indenter under load control. The indentation load was set to 3 N and the load-penetrations responses are recorded. The measured average micro Vickers hardness values in HV (taken from four different sampling points) for extruded Al and Al-MWCNT composites are listed in Table 1. The results show that the hardness values of Al-MWCNTs increase as MWCNTs weight percentage increases. Quantitatively, the increase in hardness is not so significant: about 8% increase in hardness was observed when MWCNTs weight percentage was 2.

Table 1 Properties of extruded aluminum and Al-MWCNT composites

Description	Density (g/cm^3)	Yield stress @ 0.2% off-set strain (MPa)	Ultimate tensile strength (MPa)	Average Vickers microhardness (Hv)
Aluminum	2.468 ± 0.01	90.98	98.32	68.70 ± 0.64
Al + 0.5 wt% MWCNTs	2.512 ± 0.02	114.11	121.62	70.23 ± 0.33
Al + 1.0 wt% MWCNTs	2.584 ± 0.02	138.69	151.29	71.37 ± 0.45
Al + 2.0 wt% MWCNTs	2.649 ± 0.015	176.37	184.37	74.16 ± 0.91

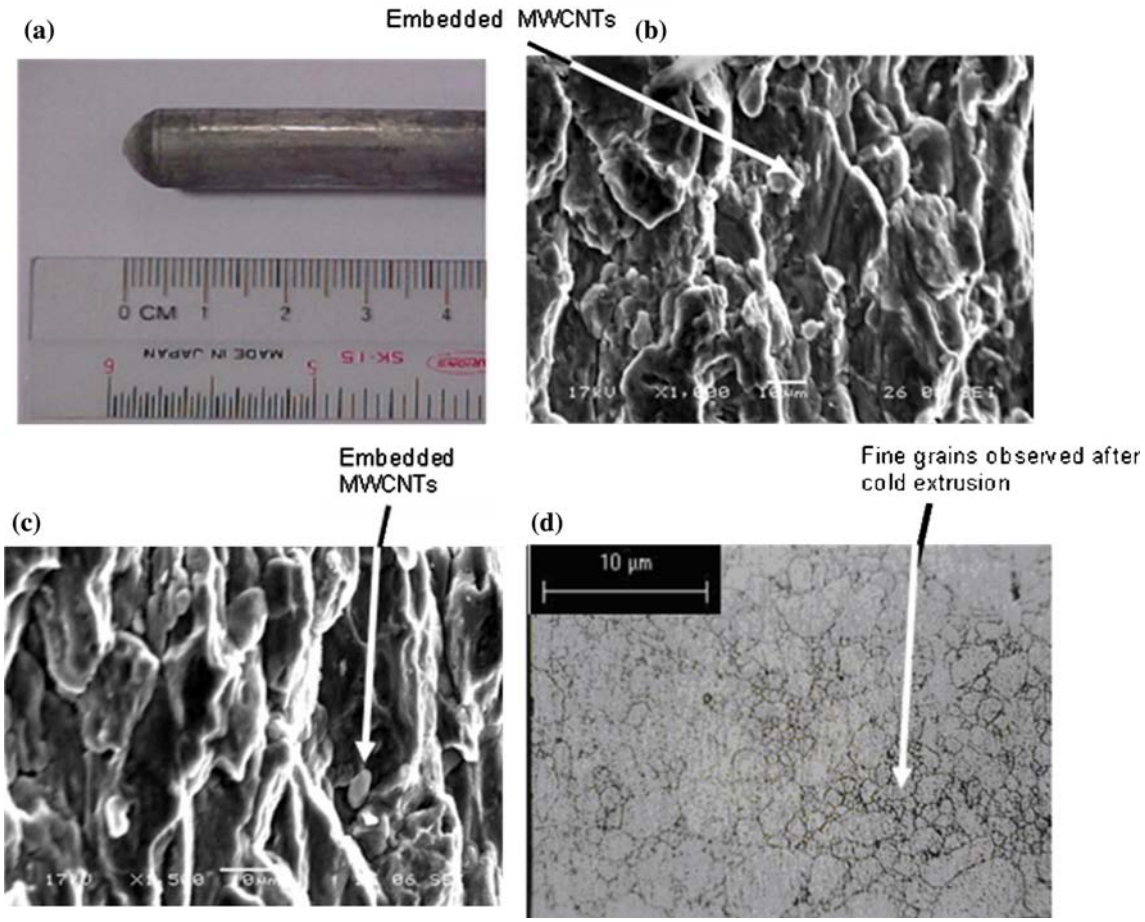

Fig. 3 **a** A photograph of extruded cylindrical AMC specimen, **b**, **c** SEM micrographs of Al-MWCNT composites showing the grain orientations and presence of MWCNTs in the extruded direction, **d** Grain size reduction observed through optical micrographs of cross-sectioned extruded aluminum sample

Uniaxial tensile tests were conducted on cylindrical specimens of 7 mm diameter and gauge length of 10 mm using a Universal Testing Machine under displacement control at 0.2 mm/min. An extensometer was used to measure the strain accurately and Instron load cell reading provided the load values. The measured uniaxial stress and strain response of pristine aluminum and Al-MWCNT composites are shown in Fig. 4. The measured 0.2% off-set yield stress and ultimate tensile strength of the composites and pristine Al samples are listed in Table 1. With increasing MWCNT weight percentage in Al matrix, the composite samples consistently showed increasing stiffness and strength, which indicates effective dispersion of MWCNTs and good interfacial bonding between the matrix and MWCNTs.

The cold extrusion step after sintering stage further densifies the part, elongates matrix grain in the axial direction, and decreases inter-particle spacing due to particle redistribution. The high strain imposed during cold extrusion leads to increase in dislocation density and to their progressive entanglement. This is the reason for strain-hardening and strengthening of cold extruded Al. Further reasoning for the increase in strength of the composite was attributed to the increased resistance to dislocation motion provided by the deformed MWCNTs

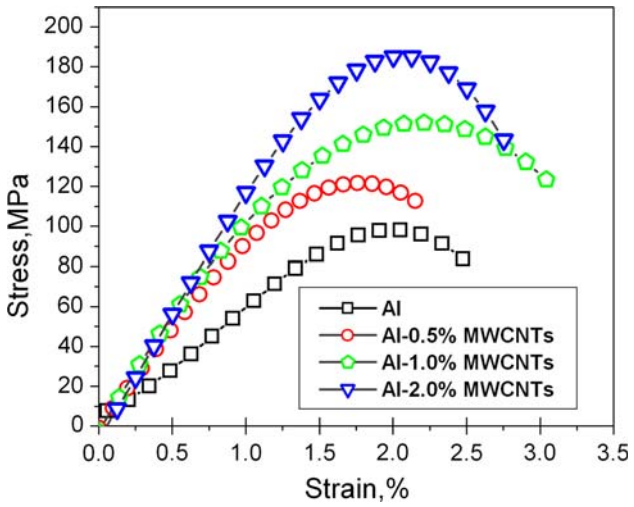

Fig. 4 Uniaxial tensile stress–strain response of pristine Al and Al-MWCNT composites

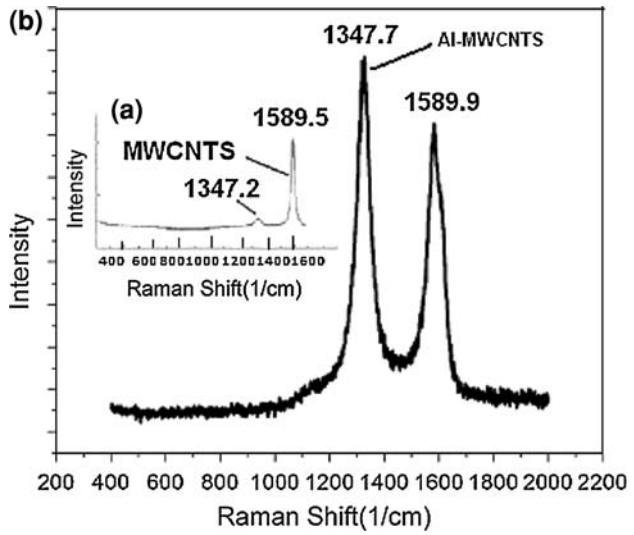

Fig. 5 Raman spectra of **a** MWCNTs after surface treatment and **b** extruded Al-MWCNT composite

during the extrusion process. This is evident from the Raman spectra shown in Fig. 5a and b for MWCNTs alone and the composite fabricated: the intensity of D-band peak becomes prominent for the composite. The deformation might even break-up the MWCNTs and hinder dislocation motion.

The yield strength and ultimate strength increased on an average approximately 90% with an addition of 2 wt% of MWCNTs. Within experimental scatter the tensile strain to fracture for the extruded samples is in-between 2 and 3%. It is to be noted that there was no further heat-treatment carried on the extruded samples. The fractured surfaces of 1 wt% Al-MWCNT composite sample are shown in Fig. 6a and we notice that even after fracture the MWCNTs were holding on to the matrix. The matrix failure is also shown in Fig. 6b.

Discussion

The mechanical characterizations of Al-MWCNT composites reveal that the adopted powder compaction route is a viable method for their manufacture. There is a consistent increase in the modulus and tensile strength of the fabricated composites with increasing weight percentage of MWCNTs. SDS seems to be an effective surfactant in dispersing the MWCNTs in Al matrix. In the following, we briefly discuss various mechanisms that have contributed to the improved mechanical behavior of Al-MWCNT composites.

George et al. [12] have elucidated three different mechanisms for the strengthening of composite materials. They include thermal mismatch, Orowan looping, and shear lag theory. Shear lag model [24] has been used to describe the stiffening effect of MWCNTs in Al-MWCNT composites. According to this theory, the Young's modulus (E_c) of the composite is given by

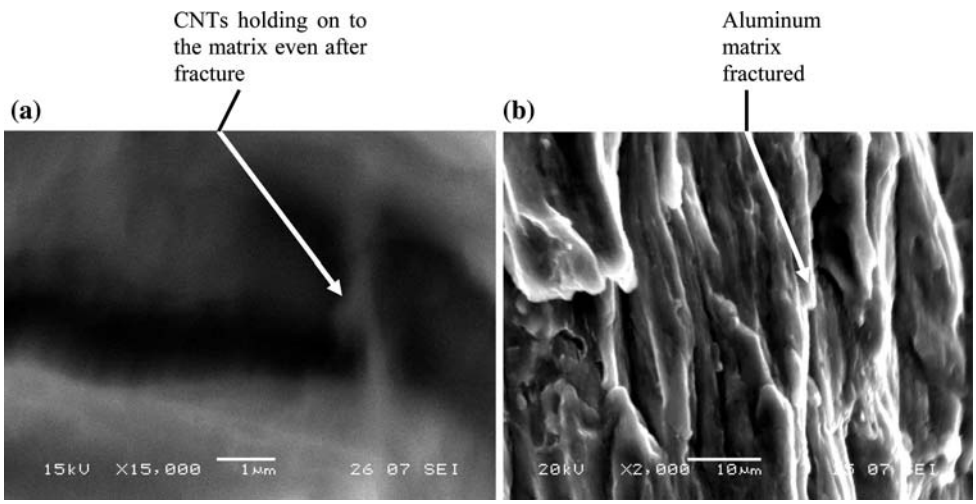

Fig. 6 **a** Fractured surface of Al/1 wt% MWCNT and **b** fracture surface fractograph

$$E_c = V_f E_f (1 - \tanh(ns))/(ns) + (1 - V_f)E_m \quad (1)$$

where $n = (2E_m/E_f(1 + \upsilon_m))\sqrt{\ln(1/V_f)}$, E_f is the Young's modulus of MWCNTs, E_m is the aluminum Young's modulus, s the aspect ratio of MWCNTs ($\sim$100), V_f the reinforcement volume fraction, and υ_m is the aluminum matrix Poisson's ratio. The modulus measured from the initial slope of the stress–strain curve is compared with the shear lag model of Eq. 1 in Table 2. Consistently the conservative upper-bound shear lag model overestimates the Young's modulus value by about 12%.

The possible reasons for the strengthening of Al-MWCNTs composites could be as follows:

1. As noted before, CNTs are nanometer dimensions: in metal matrix composites, the strengthening of metals by a given volume fraction of hard particles is greater for small particles than for large particles as it increases their rate of work-hardening.
2. During the sintering process, due to the large mismatch in the coefficient of thermal expansion between the aluminum matrix and MWCNTs results in prismatic punching of dislocations at their interface leading to the work-hardening of the aluminum matrix.
   When a stress is applied to a material the interplanar spacing (d) changes. Using Bragg's law one can determine the interplanar spacing using XRD technique. By measuring the interplanar spacing of pristine Al, Al-MWCNT composites for different incident angles of X-ray, the process-induced residual stresses can be estimated [25]. In our current experimentation, due to instrument limitations we could only measure the interplanar spacing (d) for normal incidence. The measured interplanar spacing for pristine Al was 2.3393 Å and it was 2.3252, 2.3235, and 2.3194 Å for 0.5, 1.0, and 2.0 wt% Al-MWCNTs composites, respectively. The interplanar spacing gave a relative increase in residual stresses from the extruded aluminum sample to the 2 wt% Al-MWCNT sample and showed the prominent role of MWCNTs in the strengthening of the composite by inducing lattice strains.
3. Orowan looping [26] is another strengthening mechanism in nanosized metal matrix composites. Here, the motion of the dislocations is inhibited by nanometer-sized carbon nanotubes, leading to their bending between the CNTs. This produces a back stress, which will prevent further dislocation movement leading to an increase in yield strength. The extrusion operation after the free sintering makes it difficult to make a direct comparison of composite strength with Orowan looping theory.

Table 2 Young's modulus of the specimens

Description	Experimental Young's modulus (GPa)	Shear lag Young's modulus (GPa)
Al + 0.5 wt% MWCNTs	61.92	71.97
Al + 1.0 wt% MWCNTs	66.15	74.17
Al + 2.0 wt% MWCNTs	74.62	81.95

Conclusion

Aluminum matrix composites reinforced with 0.5, 1.0, and 2.0 wt% of MWCNTs were successfully manufactured using cold compaction followed by sintering and cold extrusion techniques to near net shape. Careful controlling of sintering temperature has prevented the formation of intermetallic compounds such as aluminum carbide. The microhardness and uniaxial tensile tests have revealed enhanced mechanical properties of Al-MWCNT composites, indicating that the proposed manufacturing route is a viable cost-effective one. There was no observed percolation of MWCNTs up to the 2 wt% volume fraction. It would be further interesting to study the wear and creep properties of these composites and also explore strengthening mechanisms.

Acknowledgements The authors acknowledge many fruitful discussions they had with Prof. Raju Ramanujan and Prof. Tan Ming Jen. The experimental help rendered by Mr. Seah Kheng Wee, Mr. Lim Yee Wee, and Mr. Sa'Don Ahmad is much appreciated. The authors are grateful for the financial support from NTU Academic Research Fund (AcRF) via project number RG 19/06.

References

1. Anazawa KSK, Manabe C, Watanabe H, Shimizu M (2002) Appl Phys Lett 81:739
2. Iijima S (1991) Nature 354:56
3. Kim P, Shi L, Majumdar A, McEuen PL (2001) Phys Rev Lett 87:215502
4. Falvo MR, Clary CJ, Taylor RM, Chi V, Brooks FP, Washburn S (1997) Nature 389:582
5. Overney G, Zhong W, Tomanek D (1993) J Phys D 27:93
6. Ruoff RS, Lorents DC (1995) Carbon 33:925
7. Treacy MMJ, Ebbesen TW, Gibson JM (1996) Nature 381:678
8. Wong EW, Sheehan PE, Lieber CM (1997) Science 277:1971
9. Yakabson BI, Brabec CJ, Bernholc J (1996) Phys Rev Lett 76:2511
10. Surappa MK (2003) Sadhana 28:319
11. Deng C, Zhang X, Wang D, Lin Q, Li A (2007) Mater Lett 61:1725
12. George R, Kashyap KT, Rahul R, Yamadagni S (2005) Scr Mater 53:1159
13. Goh CS, Wei J, Lee LC, Gupta M (2006) Mater Sci Eng A 423:153
14. Shimizu Y, Miki S, Soga T, Itoh I, Todoroki H, Hosono T, Sakaki K, Hayashi T, Kim YA, Endo M, Morimoto S, Koide A (2008) Scr Mater 58:267

15. Esawi AMK, El Borady MA (2008) Compos Sci Technol 68:486
16. Tokunaga T, Kaneko K, Horita Z (2008) Mater Sci Eng A 490:300
17. Loo S, Sridhar I, Wang S, Shen L, Mhaisalkar SG (2007) Scr Mater 57:1157
18. Ventra MD, Evoy S, Heflin JR (2004) Introduction to nanoscale science and technology. Kluwer Academic Publisher, Boston
19. Xu CL, Wei BQ, Ma RZ, Liang J, Ma XK, Wu DH (1999) Carbon 13:2445
20. Zhang J, Gao L (2007) Mater Lett 61:3571
21. Jiang L, Gao L, Sun J (2003) J Colloid Interface Sci 260:89
22. Morsi K, Esawi A (2007) J Mater Sci 42:4954. doi:10.1007/s10853-006-0699-y
23. Jiang D, Thomson K, Kuntz JD, Ager JW, Mukherjee AK (2007) Scr Mater 56:959
24. Clyne TW, Withers P (1995) An introduction to metal matrix composites. Cambridge University Press, New York
25. Eigenmann B, Scholtes B, Macherauch E (1989) Mater Sci Eng A 118:1
26. Zhang Z, Chen DL (2006) Scr Mater 54:1321